AIChE WILEY InterScience DISCOVER SOMETHING GREAT

Averaging Theory for Diesel Particulate Filter Regeneration

Haishan Zheng and Jason M. Keith
Dept. of Chemical Engineering, Michigan Technological University, Houghton, MI 49931

DOI 10.1002/aic.11156
Published online March 26, 2007 in Wiley InterScience (www.interscience.wiley.com).

Axial thermal gradients play a key role in monolithic diesel particulate filters. For complete particulate regeneration, the ignition location must be near the leading edge of the diesel particulate filter. A new reduced model in terms of the capacitance-weighted and mixing cup average temperature is formulated here using the Liapunov–Schmidt reduction technique to describe the ignition behavior and account for the axial variation. The major advantage of the reduced model is that one can neglect the details of the fine scale dynamics and focus on the large scale dynamics. This new, reduced model has the ability to accurately predict two important ignition characteristics: ignition time and ignition length. Based on the reduced model results, it is shown that the thermal dispersion [a coupling of transverse diffusion (short-scale) and axial convection (long-scale)] plays a dominant role on ignition. © 2007 American Institute of Chemical Engineers *AIChE J,* 53: 1316–1324, 2007
Keywords: diesel particulate trap, reactor dynamics, modeling, ignition, reactor runaway

Introduction

Monolithic particulate filters are widely used in diesel particulate emission control. They consist of many parallel channels, which are alternately plugged at either end to force the exhaust gases through the porous ceramic walls. The particulates are deposited on the inside wall of the inlet channel to form a thin, porous soot bed. Once a sufficient mass of particulates is collected, it is burned off to regenerate the filter. Despite the great improvement in their design, diesel particulate filter (DPF) systems still experience unreliable regeneration.

Many experimental efforts have been devoted to study thermal runaway in DPF during regeneration. McCabe and Sinkevitch[1] showed that there exits a critical value for the soot temperature beyond which thermal runaway (also referred to as ignition) occurs. Furthermore, Hayashi et al.[2] and Kobashi et al.[3] have shown that ignition is necessary for complete regeneration and that regeneration can be strongly affected by the inlet gas temperature, exhaust gas flow rate, and oxygen concentration as these parameters may affect the axial location of ignition within the DPF.

Models have also been developed to predict DPF performance, most notably Bissett's one dimensional[4] and Bissett and Shadman's zero dimensional model.[5] These and other more complex models include several partial differential equations containing a very large number of physico-chemical parameters. Because of the strong coupling between the transport and reaction rate processes, the model equations are highly nonlinear. Even with the present day computational power, it is impractical to explore the different types of solutions (regeneration behaviors) for this complicated filter system. Simple correlations need to be derived for use in DPF design and control. The work presented here follows the chemical reaction engineering literature,[6–8] and in particular for automotive catalytic converters.[9–11]

Recently, Zheng and Keith[12,13] derived analytical ignition criteria (based upon Bissett and Shadman's zero dimensional model[5]] to predict the critical inlet exhaust gas temperature. This criterion is valid when the axial convection time is

Correspondence concerning this article should be addressed to J. M. Keith at jmkeith@mtu.edu.

small compared with the transverse interphase heat transfer time (high exhaust flow rates). However, the DPF is not usually operated within this range. Therefore, this manuscript focuses on the development of an accurate, low-dimensional, reduced model for this more practical case and will be used to predict DPF ignition.

Mathematical Model for the DPF

Because of the symmetry of the structure, we can consider the domain shown in Figure 1 where the axial distance down the channel is measured by z, and the transverse distance is measured by x (starting at the center of the inlet channel and ending at the center of the outlet channel). The governing equations in dimensional coordinates are described in detail in the appendix.

Using h (channel half width) and L (channel length) as the characteristic lengths in the transverse and axial directions, u_R as the reference axial velocity, k_g as the reference heat conductivity, $(\rho Cp)_g$ as the reference heat capacity, $T_R = T_{inlet}$ as the reference temperature, and r_R ($y_R T_R$) as the reference reaction rate, we obtain five time-scales in the system associated with axial convection ($t_C = L/u_R$), transverse convection ($t'_C = h/u_R$), axial thermal diffusion ($t_D = ((L^2(\rho C_p)_g)/k_g)$, transverse thermal diffusion ($t'_D = (h^2(\rho C_p)_g)/k_g$), and reaction ($t_r = ((1-\varepsilon_p)\rho_p)/(M_c r_R)$). The ratios of these time scales give rise to four dimensionless parameters: Pe (reactor scale transverse Peclet number) $= t'_D/t_C = (u_R h^2(\rho C_p)_g)/(Lk_g)$, P (axial Peclet number) $= t_D/t_C = (u_R L(\rho C_p)_g)/k_g = Pe/\Lambda^2$, P_x (local transverse Peclet number) $= t'_D/t_C = (u_R h(\rho C_p)_g)/k_g = Pe/\Lambda$, and Da (reactor scale Damköhler number) $= t_C/t_r = (LM_c r_R)/(u_R(1-\varepsilon_p)\rho_p)$, where $\Lambda = h/L$ is the aspect ratio of the monolith filter channel.

Choosing the following dimensionless variables:

$$\tau = \frac{t}{t_C}, \quad \xi = \frac{x}{h}, \quad \bar{z} = \frac{z}{L}, \quad \bar{v} = \frac{v}{u_R}, \quad \bar{u} = \frac{u}{u_R}, \quad \bar{k} = \frac{k}{k_g},$$

$$(\overline{\rho C_p}) = \frac{(\rho C_p)}{(\rho C_p)_g}, \quad \bar{r} = \frac{r}{r_R}, \quad \varsigma = \frac{E}{RT_R}, \quad \theta = \frac{E}{RT_R^2}(T - T_R),$$

$$B = \frac{E}{RT_R^2}\,\frac{(-\Delta H)(1-\varepsilon_p)\rho_p}{\left[(1-\varepsilon_p)(\rho C_p)_p + \varepsilon_p(\rho C_p)_g\right]M_c},$$

The governing equation in dimensionless form is given as

$$\bar{\alpha}\,\frac{\partial^2\theta}{\partial\xi^2} = Pe\left[\frac{\partial\theta}{\partial\tau} + \bar{u}\frac{\partial\theta}{\partial\bar{z}} - \frac{\bar{\alpha}}{P}\,\frac{\partial^2\theta}{\partial\bar{z}^2} + \frac{\gamma\bar{v}}{\Lambda}\,\frac{\partial\theta}{\partial\xi} + K\bar{r}(Y,\theta)\right] \quad (1)$$

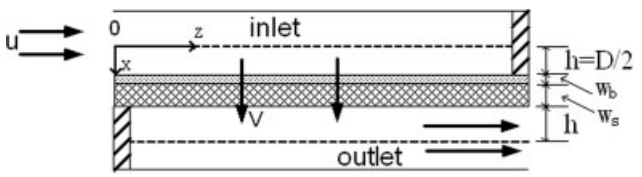

Figure 1. DPF channel.

The exhaust gas flows into the inlet channel, and is forced to flow through the porous particulate layer and substrate wall because of the closed end of the inlet channel. The exhaust gas then flows out the filter through the outlet channel.

with

$$\bar{\alpha} = \frac{\bar{k}}{(\overline{\rho C_p})} = \begin{cases} 1, & i = 1 (0 \le \xi < 1), \\ & 4 (1 + \overline{w_b} + \overline{w_s} < \xi \le 2 + \overline{w_b} + \overline{w_s}) \\ \dfrac{\overline{k_{ep}}}{(1-\varepsilon_p)\Gamma_p + \varepsilon_p}, & i = 2 (1 \le \xi < 1 + \overline{w_b}) \\ \dfrac{\overline{k_{ew}}}{(1-\varepsilon_w)\Gamma_w + \varepsilon_w}, & \\ & i = 3 (1 + \overline{w_b} \le \xi \le 1 + \overline{w_b} + \overline{w_s}) \end{cases},$$

$$\bar{u} = \begin{cases} \overline{u_1}, & i = 1 \\ 0, & i = 2, 3 \\ \overline{u_4}, & i = 4 \end{cases},$$

$$K = \begin{cases} -BDa, & i = 2 \\ 0, & \text{otherwise} \end{cases}$$

where the subscript i identifies the different phases: $i = 1$ for inlet channel ($0 \le x \le h$), $i = 2$ for the deposit layer ($h \le x \le h + w_b$), $i = 3$ for the substrate wall ($h + w_b \le x \le h + w_b + w_s$), and $i = 4$ for the outlet channel ($h + w_b + w_s \le x \le 2h + w_b + w_s$). It is noted that u_i is the axial velocity, v_i is the transverse velocity, and α_g is the gas thermal diffusivity. [Remark: the dimensional equation in vector form is given in the appendix as Eq. A4.]

The boundary conditions are:

$$\frac{\partial\theta_1}{\partial\xi} = 0 \quad \text{at } \xi = 0,$$

$$\frac{\partial\theta_4}{\partial\xi} = 0 \quad \text{at } \xi = 2 + \overline{w_b} + \overline{w_s},$$

$$\frac{\partial\theta_2}{\partial\bar{z}} = 0 \quad \text{at } \bar{z} = 0 \text{ and } \bar{z} = 1,$$

$$\frac{\partial\theta_3}{\partial\bar{z}} = 0 \quad \text{at } \bar{z} = 0 \text{ and } \bar{z} = 1,$$

$$\overline{u_1} = 0 \quad \text{at } \xi = 1,$$

$$\overline{u_4} = 0 \quad \text{at } \xi = 1 + \overline{w_b} + \overline{w_s},$$

$$\overline{u_1} = 0 \quad \text{at } \bar{z} = 1,$$

$$\overline{u_4} = 0 \quad \text{at } \bar{z} = 0,$$

$$\overline{v_1} = 0 \quad \text{at } \xi = 0,$$

$$\overline{v_4} = 0 \quad \text{at } \xi = 2 + \overline{w_b} + \overline{w_s},$$

$$\theta_1 = \theta_{inlet} \qquad \overline{u}_1 = \overline{u}_{inlet} \quad \text{at } \bar{z} = 0.$$

where $\overline{w}_b = w_b/h$ and $\overline{w}_s = w_s/h$. The initial conditions are $\theta_1 = \theta_b$ when $\tau = 0$ for all $\bar{z}$ and ξ, where θ_b is the dimensionless initial temperature.

It should be noted that the reactor scale transverse Peclet number Pe of the monolith filter is defined as the ratio of the transverse diffusion time ($(h^2(\rho C_p)_g)/k_g$) to the convection time (L/u_R) in the channels, which is small for a narrow channel and low gas flow. In the limiting case of $Pe = 0$,

the temperature is uniform throughout the transverse domain, and only the temperature gradients in the axial direction exist. This will be an important assumption in the Liapunov–Schmidt reduction which follows.

Liapunov–Schmidt Reduction

The Liapunov–Schmidt reduction technique of classical bifurcation theory has been used recently for deriving low-dimensional models for thermal and solutal dispersion problems and homogenous reactor models.[6–8,14] This technique is based on a perturbation expansion near a zero eigenvalue. After a brief review of the method, in this section we derive a new reduced model for the DPF in terms of average variables using the Liapunov–Schmidt technique.

Background

As an example, we will consider dispersion without reaction in tubular flow. It is noted that this is one of the most common geometries for reactive systems, and has application to the DPF problem considered in this manuscript. The two-dimensional Danckwerts model is frequently used in the literature, and is given by:

$$\frac{\partial C}{\partial t} + u\frac{\partial C}{\partial z} = D\left(\frac{1}{r}\,\frac{\partial}{\partial r}\left(r\frac{\partial C}{\partial r}\right) + \frac{\partial^2 C}{\partial z^2}\right) \tag{2}$$

where t is time, r is the radial direction and z is the axial direction. The system has an initial condition at $t = 0$, $C = C_o$ and boundary conditions: at $r = 0$, $r(\partial C/\partial r) = 0$, at $r = R$, $\partial C/\partial r = 0$, at $z = 0$, $u(C - C_{in}) = D(\partial C/\partial z)$, and at $z = L$, $\partial C/\partial z = 0$, where R is the tube radius and L is the tube length. The purpose of the Liapanov–Schmidt reduction technique is to reduce the dimensionality of the governing conservation equation. For the tubular flow problem described by Eq. 2, the concentration depends on time, radial position, and axial position.

The approach of the Liapunov–Schmidt reduction technique (which will be illustrated in the next subsection for the DPF) is to define cross-sectional averaged concentrations and derive, and then solve the conservation equations in terms of these average quantities. It is most common to use the average concentration $\langle C\rangle$ and the mixing-cup concentration C_m. Mathematically, these averages are given as:

$$\langle C\rangle = \frac{\int_0^R rC\,dr}{\int_0^R r\,dr} \tag{3a}$$

and

$$C_m = \frac{\int_0^R ruC\,dr}{\int_0^R ru\,dr} = \frac{\langle uC\rangle}{\langle u\rangle} \tag{3b}$$

This gives a two-mode model that recasts the Danckwerts system in Eq. 2 in terms of hyperbolic equations. Application of these averages to the two-dimensional Danckwerts model yields a system that depends only upon time and axial position:

$$\frac{\partial\langle C\rangle}{\partial t} + \langle u\rangle\frac{\partial C_m}{\partial z} = D\left(\frac{\partial^2\langle C\rangle}{\partial z^2}\right) \tag{3c}$$

$$C_m - \langle C\rangle = -\frac{D_{eff}}{\langle u\rangle}\,\frac{\partial\langle C\rangle}{\partial z} \tag{3d}$$

where D_{eff} is the effective dispersion coefficient. The initial condition is $\langle C\rangle = \langle C_0\rangle$ and the boundary conditions are given as at $z = 0$, $\langle u\rangle(C_m - C_{m,in}) = D(\partial\langle C\rangle/\partial z)$ and at $z = L$ as $\partial\langle C\rangle/\partial z = 0$. This method is only valid after the transverse diffusion timescale, R^2/D has elapsed. However, it is noted that the model is of reduced dimension and offers more rapid simulation and the possibility of analytical solutions if there are some relaxed kinetic approximations, a strong advantage of the Liapunov–Schmidt reduction technique. This approach can also be used to appropriately separate disparate time and length scales that often arise in modern chemical engineering problems.

It is noted that the theoretical development is described in more detail within mainstream chemical engineering publications by the group of Balakotaiah,[6–8,14] and in the interest of brevity is not shown here. In the following sub-section we will utilize this theory for the DPF.

Application to the DPF

The analysis begins by assuming negligible deposit consumption prior to ignition. With this assumption, the mass balance equation for the deposit layer can be neglected. The transverse domain Ω is defined as $0 \le \xi \le 2 + \overline{w}_b + \overline{w}_s$, and the linear operator £ over the domain Ω is defined as

$$£\theta \equiv \bar{\alpha}\Delta\theta \tag{4}$$

where the operator Δ is the Laplacian operator for the transverse direction ($\Delta = \partial^2/\partial\xi^2$). The thermal coefficients $\bar{\alpha}$ are constant in each phase, but vary from phase to phase and are hence functions of the transverse coordinate ξ.

Equation 1 is rewritten as

$$F(\theta, Pe) \equiv £\theta - Pe\left[\frac{\partial\theta}{\partial\tau} + \bar{u}\frac{\partial\theta}{\partial\bar{z}} - \frac{\bar{\alpha}}{P}\,\frac{\partial^2\theta}{\partial\bar{z}^2} + \frac{\gamma\bar{v}}{\Lambda}\,\frac{\partial\theta}{\partial\xi} + K\bar{r}(\theta)\right] = 0 \tag{5}$$

[Remark: Even though the reaction rate $\bar{r}$ is a function of y, for simplicity it is not written in Eq. 5. This system will be solved with the usual assumption of negligible reactant consumption in classical ignition theory. Thus, a balance equation for the particulate deposit is not presented here. This assumption will be described in more detail in a subsequent section.] This operator £ (with Neumann boundary conditions $\partial\theta/\partial\xi = 0$ at $\xi = 0$ and $\xi = 2 + \overline{w}_b + \overline{w}_s$) is symmetric and has a zero eigenvalue with a constant null eignenfunction ϕ_0, which can be chosen as unity. The average operator $\langle\bullet\rangle$ is defined as

$$\langle\omega\rangle = [\omega, \phi_0] = \frac{1}{\Omega_{C_p}} \int_0^{2+\overline{w}_b+\overline{w}_s} (\overline{\rho C_p})\omega d\xi \tag{6}$$

where $\Omega_{C_p} = \int_0^{2+w_b+\overline{w_s}} (\overline{\rho C_p}) d\xi$ is the total capacitance of the system. Using this concept, θ can be expressed as

$$\theta = \langle\theta\rangle + \theta' \tag{7}$$

where $\langle\theta\rangle$ is the capacitance-weighted average temperature and θ' is the perturbation of the local temperature θ from $\langle\theta\rangle$. Because of the Neumann boundary conditions on θ, it follows that

$$\langle \pounds\theta\rangle = 0 \text{ and } \langle\theta'\rangle = 0 \tag{8}$$

Applying Eq. 6 to Eq. 5 and invoking the dimensionless mass continuity equation yields:

$$\frac{\partial\langle\theta\rangle}{\partial\tau} + \langle\bar{u}\rangle\frac{\partial\theta_m}{\partial\bar{z}} - \frac{1}{P}\frac{\partial^2\langle\bar{\alpha}\theta\rangle}{\partial\bar{z}^2} + \langle K\bar{r}(\theta)\rangle = 0 \tag{9}$$

where $\theta_m = \langle\bar{u}\theta\rangle/\langle\bar{u}\rangle$ is the mixing cup average temperature.

We note that the axial heat conduction term in the averaged equation is order of 1/P. The value of $P = Pe/\Lambda^2$ can be very large for a narrow channel even when the value of Pe is small. In the monolith filter problem, the value of Λ ($\Lambda \sim 0.004$) is far smaller than the value of Pe ($Pe \sim 0.3$). Therefore, P is far greater than unity. It should also be noted that the dimensionless thermal diffusivity is also small ($\alpha = 1$ for the gas, and $\bar{\alpha} \sim 0.03$ for the particulate matter and ceramic wall). Other terms in Eq. 9 are of unit order. This shows that the axial heat conduction is unimportant, especially in the ignition phenomenon, and thus can be safely omitted. Therefore, Eq. 9 becomes

$$\frac{\partial\langle\theta\rangle}{\partial\tau} + \langle\bar{u}\rangle\frac{\partial\theta_m}{\partial\bar{z}} + \langle K\bar{r}(\theta)\rangle = 0 \tag{10}$$

and will be referred to as the "averaged equation."

Equation 5 can be solved with by using a perturbation expansion of θ' in the small parameter Pe, such that

$$\theta' = Pe\theta_1 + Pe^2\theta_2 + \cdots, \tag{11}$$

One obtains the trivial solution $\pounds\langle\theta\rangle = 0$ at order unity and

$$\pounds\theta_1 = \frac{\partial\langle\theta\rangle}{\partial\tau} + \bar{u}\frac{\partial\langle\theta\rangle}{\partial\bar{z}} + K\bar{r}(\langle\theta\rangle) \tag{12}$$

at order Pe. It is worthwhile to point out that Eq. 12 shows that at leading order the thermal dispersion is caused only by the nonuniform axial convection and reaction in the transverse direction. The dispersion effects because of the transverse convective flow are captured at order Pe^2 and higher. When the value of Pe is large, the expansion must be carried to higher orders in Pe so that the reduced model can capture the effect of the transverse convection.

The mixing-cup average temperature θ_m and capacitance-weighted average temperature $\langle\theta\rangle$ are equal at leading order, since

$$\theta_m = \langle\theta\rangle + Pe\frac{\langle\bar{u}\theta_1\rangle}{\langle\bar{u}\rangle} + O(Pe^2). \tag{13}$$

The reaction rate can be determined from the Taylor series

$$\bar{r}(\theta) = \bar{r}(\langle\theta\rangle + \theta') \sim \bar{r}(\langle\theta\rangle) + \frac{d\bar{r}}{d\theta}(\langle\theta\rangle)\theta', \tag{14}$$

Solving the "averaged equation" for $\partial\langle\theta\rangle/\partial\tau$, and then inserting the results into Eq. 12 yields at leading order:

$$\pounds\theta_1 = (\bar{u} - \langle\bar{u}\rangle)\frac{\partial\langle\theta\rangle}{\partial\bar{z}} + (K - \langle K\rangle)\bar{r}(\langle\theta\rangle) \tag{15}$$

If parameters η and χ are now defined according to

$$\pounds\eta = \bar{u} - \langle\bar{u}\rangle, \tag{16}$$

$$\pounds\chi = K - \langle K\rangle. \tag{17}$$

one obtains

$$\theta_1 = \eta\frac{\partial\langle\theta\rangle}{\partial\bar{z}} + \chi\bar{r}(\langle\theta\rangle) \tag{18}$$

Equations 16 and 17 are referred to as the "local equations" and show that η is caused by the gas velocity gradient in the transverse direction, and χ is caused by the nonuniform reaction rate in the transverse direction. It should be pointed out that η and χ both satisfy the continuity conditions at the interface between different phases, and the no flux condition at the boundary of the domain Ω. Furthermore, the conditions $\langle\eta\rangle = 0$ and $\langle\chi\rangle = 0$ must hold true as $\langle\theta_1\rangle = 0$.

To leading order, the reduced model is obtained by substituting Eqs. 14 and 18 into Eq. 10:

$$\frac{\partial\langle\theta\rangle}{\partial\tau} + \langle\bar{u}\rangle\frac{\partial\theta_m}{\partial\bar{z}} + \langle K\rangle\bar{r}(\langle\theta\rangle) + Pe\frac{d\bar{r}}{d\theta}(\langle\theta\rangle)\left[\langle K\eta\rangle\frac{\partial\langle\theta\rangle}{\partial\bar{z}} + \langle K\chi\rangle\bar{r}(\langle\theta\rangle)\right] = 0 \tag{19a}$$

Furthermore, substitution of Eq. 18 into Eq. 13 gives

$$\theta_m - \langle\theta\rangle = Pe\left[\frac{\langle\bar{u}\eta\rangle}{\langle\bar{u}\rangle}\frac{\partial\langle\theta\rangle}{\partial\bar{z}} + \frac{\langle\bar{u}\chi\rangle}{\langle\bar{u}\rangle}\bar{r}(\langle\theta\rangle)\right] \tag{19b}$$

We will solve these equations in subsequent sections of this article. At this juncture, it is worthwhile to point out that the two local constants in Eq. 19b ($\langle\bar{u}\eta\rangle/\langle\bar{u}\rangle$ and $\langle\bar{u}\chi\rangle/\langle\bar{u}\rangle$) represent thermal dispersion effect because of axial velocity gradients in the transverse direction, and the two local constants in Eq. 19a ($\langle K\eta\rangle$ and $\langle K\chi\rangle$) represent thermal dispersion effects because of a nonuniform reaction.

Derivation of the Reduced Thermal Model

In this section the local constants are determined. To begin, the functions η and χ are obtained by solving the local Eqs. 16 and 17. Opris and Johnson[15] have shown that a Poiseuille type flow can be assumed in the z-direction. For simplicity, assuming the transverse velocity is independent of axial distance yields the following velocity profiles in the inlet channel:

$$\bar{u}_1 = \frac{3}{2}(1-\bar{z})(1-\xi^2) \tag{20a}$$

$$\bar{v}_1 = \frac{\Lambda}{2}(3\xi - \xi^3) \tag{20b}$$

By mass continuity, a similar velocity profile can be obtained for the outlet channel. The axial velocity distribution is thus given by:

$$\bar{u} = \begin{cases} \frac{3}{2}(1-\bar{z})(1-\xi^2), & i = 1(0 \le \xi \le 1) \\ 0, & i = 2,3(1 \le \xi \le 1 + \bar{w}_b + \bar{w}_s) \\ \frac{3}{2}\bar{z}\,[1-(2+\bar{w}_b+\bar{w}_s-\xi)^2], & \\ & i = 4(1+\bar{w}_b+\bar{w}_s \le \xi \le 2+\bar{w}_b+\bar{w}_s) \end{cases} \tag{21}$$

The transverse velocity distribution can also be derived but is not needed at order Pe in the Liapunov–Schmidt reduction method presented in Eq. 19 above.

The cross-sectional average velocity is given as:

$$\langle \bar{u} \rangle = \frac{1}{\Omega_{C_p}} \int_{\Omega} (\overline{\rho C_p}) \bar{u} d\Omega = \frac{1}{\delta} \tag{22}$$

where $\delta = 2 + \overline{w}_b[(1-\varepsilon_p)\Gamma_p + \varepsilon_p] + \overline{w}_s[(1-\varepsilon_w)\Gamma_w + \varepsilon_w]$. Also, the cross-sectional averaged reaction rate is given as:

$$\langle K \rangle = \frac{1}{\Omega_{C_p}} \int_{\Omega} \overline{\rho C_p} K d\Omega = -\sigma_p BDa \tag{23}$$

with

$$\sigma_p = \frac{[(1-\varepsilon_p)\Gamma_p + \varepsilon_p]\bar{w}_b}{\delta}$$

representing the ratio of the heat capacity of the deposit layer to the total heat capacity of the filter. The value of σ_P is determined by the initial loading and is an important and easily controlled design parameter in DPF regeneration.

To simplify the calculation of η and χ, constant values of η and χ at the solid phase $(1 < \xi < 1 + \overline{w}_b + \overline{w}_s)$ are assumed in the thin, transverse direction because of a short heat conduction timescale. A uniform solid phase temperature in the ξ direction is the common assumption which has been used in many 1D DPF models.[4,16] With this assumption in mind, Eqs. 16 and 17 can be solved to yield:

$$\eta = \begin{cases} (1-z)\left(\frac{3}{4}\xi^2 - \frac{1}{8}\xi^4\right) - \frac{1}{2\delta}\xi^2 & \\ \qquad + \frac{9}{10\delta} - \frac{2}{3\delta^2} - \frac{5}{8}(1-\bar{z}), & 0 \le \xi \le 1 \\ \frac{2}{5\delta} - \frac{2}{3\delta^2}, & 1 \le \xi \le H-1 \\ z\left[\frac{3}{4}(H-\xi)^2 - \frac{1}{8}(H-\xi)^4\right] - \frac{1}{2\delta}(H-\xi)^2 & \\ \qquad + \frac{9}{10\delta} - \frac{2}{3\delta^2} - \frac{5}{8}\bar{z}, & H-1 \le \xi \le H \end{cases} \tag{24}$$

$$\chi = \begin{cases} \frac{\sigma_p BDa}{2}\xi^2 + \left(\frac{2}{3\delta} - \frac{1}{2}\right)\sigma_p BDa, & 0 \le \xi \le 1 \\ \frac{2}{3\delta}\sigma_p BDa, & 1 \le \xi \le H-1 \\ \frac{\sigma_p BDa}{2}(H-\xi)^2 + \left(\frac{2}{3\delta} - \frac{1}{2}\right)\sigma_p BDa, & H-1 \le \xi \le H \end{cases} \tag{25}$$

where $H = 2 + \overline{w}_b + \overline{w}_s$.

These expressions can be used to determine the local constants as:

$$\langle u\eta \rangle = \frac{1}{\delta} f(\bar{z}) = \frac{1}{\delta}\left\{\frac{4}{5\delta} - \frac{2}{3\delta^2} - \frac{17}{35}[(1-\bar{z})^2 + \bar{z}^2]\right\} \tag{26a}$$

$$\langle u\chi \rangle = \frac{\sigma_p BDa}{\delta}\left(\frac{2}{3\delta} - \frac{2}{5}\right) \tag{26b}$$

$$\langle K\chi \rangle = -\frac{2}{3\delta}(\sigma_p BDa)^2 \tag{26c}$$

$$\langle K\eta \rangle = \frac{\sigma_p BDa}{\delta}\left(\frac{2}{3\delta} - \frac{2}{5}\right) \tag{26d}$$

which can be substituted into Eq. 19. The initial conditions for $\langle\theta\rangle$ and θ_m are simply the capacitance weighted average and mixing cup average of the initial conditions of θ,

$$\langle\theta\rangle(\tau = 0) = \theta_m(\tau = 0) = \theta_{inlet} \tag{27}$$

The Danckwerts boundary condition can be derived from Eq. 19b and the inlet condition:

$$\theta_{m0} - \langle\theta\rangle = Pe\left\{\frac{4}{5\delta} - \frac{2}{3\delta^2} - \frac{17}{35}\,[(1-\bar{z})^2 + \bar{z}^2]\right\}\frac{\partial\langle\theta\rangle}{\partial\bar{z}} \tag{28}$$

where θ_{m0} is the mixing cup average of inlet temperature. It is noted that the reduced model Eqs. 19 and 26 shows that the system behavior determined by three constants: the transverse Peclet number Pe, the total heat capacity δ, and the product $\sigma_p\ BDa$ (product of the ratio of heat capacity of the deposit layer over the total heat capacity σ_p, the dimensionless adiabatic temperature rise B, and the reactor scale Damköhler number Da). It is noted that when σ_p is equal to zero, the reduced model collapses into to the classical convection and diffusion model without reactions.

Comparison with the Full 1D Model

In this section, the simulation results of the reduced model are compared with that of the classical Bissett 1D full model[4] in terms of the ignition time and ignition length for different inlet temperatures. Pertinent physical property data and channel parameters used in our simulations is available in Table 1. When using a reproduction of the Bissett model, a plot of the regeneration efficiency (deposit consumption divided by initial loading) vs. time is created for each inlet temperature. The ignition time is defined by extrapolating this efficiency vs. time graph to zero efficiency, as seen in the example of Figure 2. Also, the ignition length is defined as the first point at which the local thickness of

Table 1. Physical Properties and Operating Parameters

Gas parameters	
P	1.013×10^5 (Pa)
C_{pg}	1.17 (J/g K)
k_g	2.38×10^{-2} (W/m K)
R_{gas}	8.314 (J/mol K)
M_{air}	28.5 (g/mol)
ρ_g	$\rho_g = PM_{air}/R_{gas}T_{in}$ (g/cm^3)
G_f	0.272 (g/cm^2 s)
u_R	$u_R = G_f/2\rho_g$ (cm/s)
y_f	0.154
T_o	600 K
Monolith parameters	
D	0.211 (cm)
L	25.4 (cm)
w_s	4.76×10^{-2} (cm)
ε_w	0.5
ρ_w	2.58 (g/cm^3)
C_{pw}	1.11 (J/g K)
k_w	2.1 (W/m K)
Carbon (deposit) parameters	
C_{pp}	1.51 (J/g K)
r_p	0.55 (g/cm^3)
k_p	0.84 (W/m K)
ε_p	0.5
ΔH	-3.93×10^5 (J/mol)
E/R	1.8×10^4 (K)
Averaged model parameters (dimensionless quantities)	
β	$1 + T_{inlet}/18{,}000$
σ_p	0.0134
B	$3.905 \times 10^8/T_{inlet}^2$
Da	$1.041 \times 10^8 \exp(-18{,}000/T_{inlet})$
Pe	0.342
δ	1.038×10^3

the deposit layer decreases to zero. For the reduced model, a plot of the maximum temperature vs. time is utilized so that the ignition length is estimated at the location of maximum temperature. Figure 3 shows an example of estimating the ignition time using the reduced model.

Comparison between a reproduction of the Bissett model[4] with that of the reduced model (this work) is shown in Figure 4 for the ignition time and Figure 5 for the ignition length. It can be seen that there is a very good agreement. The reduced model has some error (less than 10%) for the case of downstream ignition. This is likely due to the assumption of negligible reactant consumption before ignition. Reproductions of the Bissett[4] model show modest reduction in the deposit layer thickness prior to ignition. The model appears to perform better when the ignition is closer to the leading edge, when there is little reactant consumption before ignition.

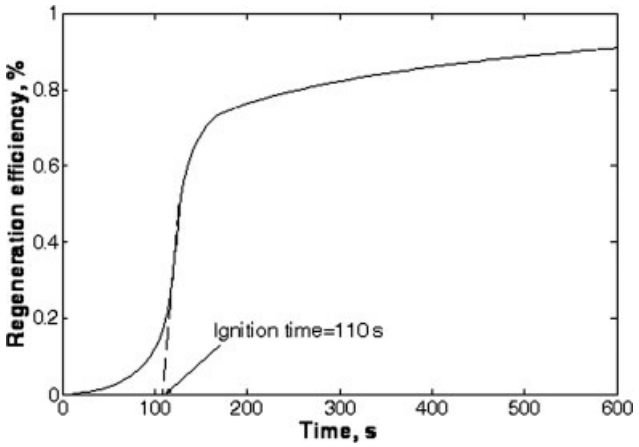

Figure 2. The regeneration efficiency as a function of time.

The data are calculated from a reproduction of Bissett's 1D model[4] for an inlet temperature 660 K. Other conditions are taken from Table 1.

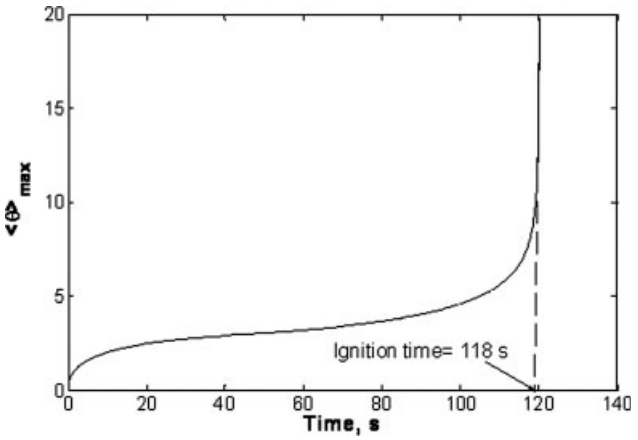

Figure 3. The maximum capacitance-weighted average temperature as a function of time.

The data are calculated from the reduced model for an inlet temperature 660 K. Other conditions are taken from Table 1.

Analytical Ignition Time

In this section, the reduced model will be used to derive an analytical expression for the ignition time. Furthermore, the influence of various parameters on ignition will be discussed.

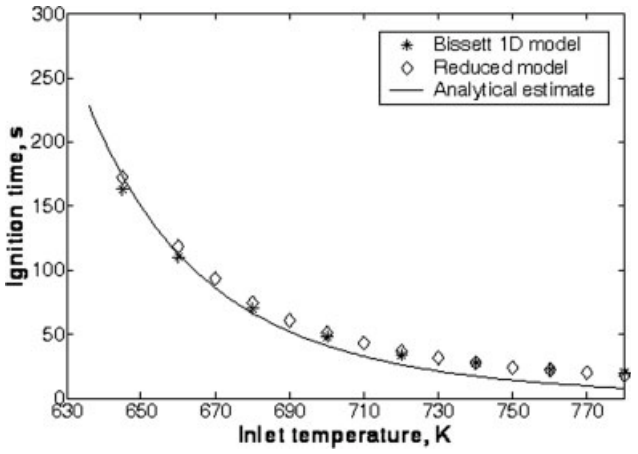

Figure 4. The ignition time as a function of the inlet temperature.

Simulation data, plotted as diamonds, are taken from the reduced model. Simulation data, plotted as stars, are taken from a reproduction of the model of Bissett.[4] The analytical estimate of Eq. 32 is plotted as a solid line.

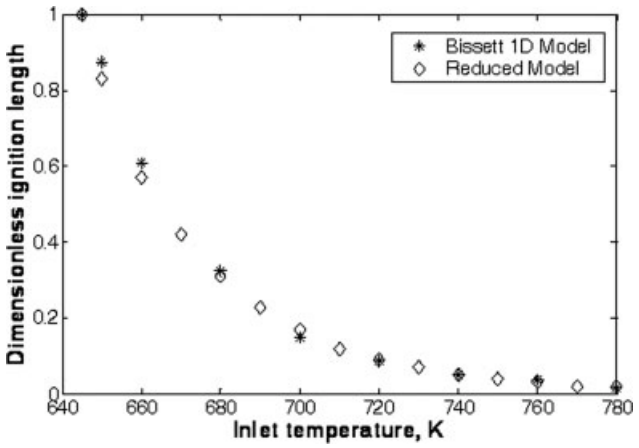

Figure 5. The dimensionless ignition length as a function of the inlet temperature.

Simulation data, plotted as diamonds, are taken from the reduced model. Simulation data, plotted as stars, are taken from a reproduction of the model of Bissett.[4]

Substitution of Eq. 19b into Eq. 19a and keeping terms of O(Pe) gives

$$\frac{\partial\langle\theta\rangle}{\partial\tau}+U_{\text{eff}}\frac{\partial\langle\theta\rangle}{\partial\bar{z}}=\alpha_{\text{eff}}\frac{\partial^2\langle\theta\rangle}{\partial\bar{z}^2}+K_{\text{eff}}\bar{r}(\langle\theta\rangle) \tag{29}$$

which is valid after the two modes (average temperature and mixing-cup temperature) are in thermal equilibrium, usually after $\tau>t'_{\text{d}}/t_{\text{c}}=Pe$. In Eq. 29, the effective velocity, thermal dispersion, and reaction rate are given by:

$$u_{\text{eff}}=\frac{1}{\delta}\left\{1+Pe\left[g(\bar{z})+\left(\frac{4}{3\sigma}-\frac{4}{5}\right)\sigma_{\text{p}}BDa\frac{d\bar{r}}{d\theta}(\langle\theta\rangle)\right]\right\},$$

$$\alpha_{\text{eff}}=-Pe\frac{f(\bar{z})}{\delta}$$

$$K_{\text{eff}}=\sigma_{\text{p}}BDa\left[1+Pe\frac{2\sigma_{\text{p}}BDa\frac{d\bar{r}}{d\theta}(\langle\theta\rangle)}{3\delta}\right],$$

with

$$f(\bar{z})=\frac{4}{5\delta}-\frac{2}{3\delta^2}-\frac{17}{35}[(1-\bar{z})^2+\bar{z}^2],$$

$$g(\bar{z})=\frac{\partial f}{\partial\bar{z}}=-\frac{34}{35}(2\bar{z}-1).$$

Equation 29 is similar to the classical convection-diffusion-reaction model of packed-bed reactors. The new feature that appears in the DPF regeneration problem is the presence of corrections to the velocity U_{eff} and source term K_{eff}. However, as these factors are of order Pe (note that $Pe\ll 1$ for the DPF) one obtains to leading order $U_{\text{eff}}=1/\delta$ and $K_{\text{eff}}=\sigma_{\text{p}}\ BDa$. Finally, the dispersion coefficient α_{eff} is a weak function of $\bar{z}$ ($f(\bar{z})$ has a maximum value of -0.25 at $\bar{z}=0.5$, and minimum value of -0.49 at $\bar{z}=0$ or 1), and will be replaced here with the average value of -0.32 to obtain an analytical estimate.

To get an explicit equation for ignition time, the reaction kinetics are reduced to a zero order Frank–Kamenetskii form given by $\bar{r}(\langle\theta\rangle)\sim \text{A}\exp[\beta(\langle\theta\rangle-\langle\theta\rangle_{\text{inlet}})]$. The dimensionless reaction rate, assuming constant oxygen concentration throughout the deposit layer, is given as

$$\bar{r}=\frac{k(T)}{k(T_{\text{R}})}=\frac{T}{T_{\text{R}}}\exp\left(-\frac{E}{R}\left(\frac{1}{T}-\frac{1}{T_{\text{R}}}\right)\right)$$

In terms of $\theta=E/(RT_{\text{R}}^2)(T-T_{\text{R}})$ and $\varsigma=E/(RT_{\text{R}})$ this can be written as

$$\bar{r}(\theta)=\left(1+\frac{\theta}{\varsigma}\right)\exp\left(\frac{\theta}{1+\theta/\varsigma}\right)$$

The values of A and β, depending on the initial conditions, can be calculated from the equations $A=\bar{r}(\theta=0)=1$ and $\beta=d\bar{r}/d\theta(\theta=0)=1+\frac{1}{\varsigma}$, respectively.

Furthermore, defining the parameters $\upsilon=\beta(\langle\theta\rangle-\langle\theta\rangle_{\text{in}})$, $\tau'=(U_{\text{eff}}^2/\alpha_{\text{eff}})\tau$, $y=(U_{\text{eff}}/\alpha_{\text{eff}})\bar{z}$, $\psi=(\alpha_{\text{eff}}K_{\text{eff}}A\beta)/U_{\text{eff}}^2$, and $\eta=-\beta\ \langle\theta_{\text{inlet}}\rangle$ yields:

$$\frac{\partial\upsilon}{\partial\tau'}+\frac{\partial\upsilon}{\partial y}=\frac{\partial^2\upsilon}{\partial^2 y}+\psi e^{\upsilon} \tag{30}$$

This equation has been solved analytically by Leighton and Chang[9] to predict the ignition time (time for the temperature to reach infinity) for small values of the parameter ψ. They indicated that a downstream ignition will take place at the point just behind the thermal boundary layer that propagates into the reactor (in this case the DPF). Their expression is given as:

$$\tau'\psi=1+2\sqrt{\psi}\left|\ln(\sqrt{\psi}/2\eta)\right|^{1/2} \tag{31}$$

or in terms of the original dimensionless variables:

$$\tau_{\text{ig}}=\frac{1}{\beta\sigma_{\text{p}}BDa}\left\{1+1.14\sqrt{\beta\sigma_{\text{p}}BDaPe\delta}\times\left|\ln(0.28\sqrt{\beta\sigma_{\text{p}}BDaPe\delta}/(-\beta\langle\theta_{\text{inlet}}\rangle))\right|^{1/2}\right\} \tag{32}$$

Equation 32 has been derived with two major approximations: negligible reactant consumption and a zero order reaction rate approximation (Frank–Kamenetskii or positive exponential approximation). A comparison between the full one dimensional model and the analytical solution is shown in Figure 4. This is an appropriate comparison since 1D and 2D DPF models have shown excellent agreement.[17] Figure 4 also shows the reduced model for completeness. There is excellent comparison for the case of downstream ignition.

We note that as the parameter ψ is increased to unit order, the ignition location moves upstream towards the leading edge of the DPF, and Eq. 30 breaks down. This results in a prediction of a faster ignition. Figure 4 shows that when the inlet temperature is greater than 750 K, there is about a 5–8 s difference in the ignition time.

However, ignition occurs at the leading edge of channel for inlet temperature above 750 K. After ignition, the thermal

front moves downstream because of convective flow, and thus ignites the remaining particulate soot in sequence. Therefore, 750 K is high enough to obtain a complete regeneration, A higher inlet temperature will not improve regeneration performance but increase the fuel penalty. This analytical estimate can be used with confidence for most operating conditions.

Conclusions

A new reduced model is derived here by averaging a 2D thermal model based on the Liapunov–Schmidt technique. This reduced model is expressed in terms of two average temperature variables (the capacitance weighted average temperature and the mixing cup average temperature) and two coupled equations for these variables. It has been shown that this reduced model has a very good agreement with the classic Bissett 1D model in the prediction of the ignition behavior (ignition time and ignition length). It should be noted that this reduced model is effective only when the transverse diffusion time is much smaller than the axial convection time. This requirement is usually satisfied in the case of low exhaust flow rates.

Several assumptions have been made to derive the reduced model: negligible soot consumption, constant oxygen concentration, and constant transverse flow in the solid phase. It should be noted that these assumptions are applicable only before ignition. They introduce little error to describe the ignition behavior in the reduced model.

It is worth mentioning that the thermal dispersion, a coupling of the transverse diffusion (short-scale) and axial convection (long-scale), is the dominant effect [order of $O(Pe)$] for the ignition phenomena. Axial heat conduction is much smaller compared with the axial thermal dispersion, thus it is safely omitted in the reduced model. The short scale (transverse) convection, which is the unique characteristic for the filter problem, is captured in the term of order Pe^2. When the value of Pe is very small, the transverse convection can be safely neglected.

The reduced model presented here can be used to perform analytical analyses of the ignition behavior in DPF system. An analytical equation (Eq. 32) has been derived here from the reduced model by reducing the reaction kinetics to a Frank–Kamenetskii form. The analytical equation is in very good agreement with numerical solutions of the full model and the reduced model in terms of ignition time, and provides an easy way to predict the ignition time which is a key parameter for designing, controlling, and optimizing DPF systems.

Acknowledgments

The authors thank the financial support from a 3M Nontenured Faculty Grant as well as the College of Engineering and Graduate School at MTU. Discussion with Dr. Jason Yang of Michigan Technological University is also noted.

Literature Cited

1. McCabe RW, Sinkevitch RM. A Laboratory combustion study of diesel particulates containing metal additives. *Soc Auto Eng*. 1986; 95:72–84. SAE Paper No. 860011.
2. Hayashi K, Ogura Y, Kobashi K, Sami H, Fukami A. Regeneration capability of wall-flow monolith diesel particulate filter with electric heater. *Proc Soc Automot Eng 1990. World Congress*. SAE Paper No. 900603.
3. Kobashi K, Hayashi K., Aoki H, Kurazono K, Fujimoto M. Regeneration capability of diesel particulate filter system using electric heater. *Proc Soc Automot Eng 1993. World Congress*. SAE Paper No. 930365.
4. Bissett EJ. Mathematical model of the thermal regeneration of a wall-flow monolith diesel particulate filter. *Chem Eng Sci*. 1984;39: 1233–1244.
5. Bissett EJ, Shadman F. Thermal regeneration of diesel particulate monolithic filters. *AIChE J*. 1985;31:753–758.
6. Chakraborty S, Balakotaiah V. Low dimensional models for describing mixing effects in laminar flow tubular reactors. *Chem Eng Sci*. 2002;57:2545–2564.
7. Chakraborty S, Balakotaiah V. Two-mode models for describing mixing effects in homogenous reactors. *AIChE J*. 2002;48:2571–2586.
8. Balakotaiah V, Charkraborty S. Averaging theory and low-dimensional models for chemical reactors and reacting flows. *Chem Eng Sci*. 2003;58:4769–4786.
9. Leighton DT, Chang HC. A theory for fast-igniting catalytic converters. *AIChE J*. 1995;41:1989–1914.
10. Keith JM, Chang HC, Leighton DT. Designing a fast-igniting catalytic converter system. *AIChE J*. 2001;47:650–663.
11. Ramanathan K, Balakotaiah V, West DH. Light-off criterion and transient analysis of catalytic monoliths. *Chem Eng Sci*. 2003;58: 1381–1405.
12. Zheng H, Keith JM. A new design for efficient diesel particulate trap regeneration. *AIChE J*. 2004;50:184–191.
13. Zheng H, Keith JM. Ignition analysis of wall-flow monolith diesel particulate filters. *Catal Today*. 2004;98:403–412.
14. Balakotaiah V, Chang HC. Hyperbolic homogenized models for thermal and solutal dispersion. *SIAM J Appl Math*. 2003;63:1231–1258.
15. Opris CN, Johnson JH. A 2-D computational model describing the heat transfer, reaction kinetics and regeneration characteristics of a ceramic diesel particulate trap. *Proc Soc Automot Eng 1998. World Congress*. SAE Paper No. 980546.
16. Huynh CT, Johnson JH. Yang SL, Bagley ST, Warner JR. A one-dimensional computational model for studying the filtration and regeneration characteristics of a catalyzed wall-flow diesel particulate filter. *SAE 2003 Trans J Fuels Lubricants*. 2004;112(4):620–646.
17. Zhang Z, Yang SL, Johnson JH. Modeling and numerical simulation of diesel particulate trap performance during loading and regeneration. *SAE 2002 Trans J Fuels Lubricants*. 2003;111:471–483.

Appendix: Governing Equations

The energy equation in the inlet/outlet channel is a two dimensional partial differential equation which includes the heat accumulation term, axial and transverse convection, and axial and transverse heat conduction, written in terms of the temperature T:

$$\frac{\partial T_{\mathrm{i}}}{\partial t} + u_{\mathrm{i}} \frac{\partial T_{\mathrm{i}}}{\partial z} + v_{\mathrm{i}} \frac{\partial T_{\mathrm{i}}}{\partial x} = \alpha_{\mathrm{g}} \left(\frac{\partial^2 T_{\mathrm{i}}}{\partial z^2} + \frac{\partial^2 T_{\mathrm{i}}}{\partial x^2} \right) \qquad \text{(A1)}$$

where the subscript i identifies the different phases: $i = 1$ for inlet channel ($0 \le x \le h$), $i = 2$ for the deposit layer ($h \le x \le h + w_{\mathrm{b}}$), $i = 3$ for the substrate wall ($h + w_{\mathrm{b}} \le x \le h + w_{\mathrm{b}} + w_{\mathrm{s}}$), and $i = 4$ for the outlet channel ($h + w_{\mathrm{b}} + w_{\mathrm{s}} \le x \le 2h + w_{\mathrm{b}} + w_{\mathrm{s}}$). In Eq. 1, u_i is the axial velocity, v_i is the transverse velocity, and α_{g} is the gas thermal diffusivity.

It should be noted that the gas temperature equilibrates much more rapidly than the solid temperature in the DPF. Therefore, a quasi-steady state approximation for the exhaust

flow in the channel can be used. However, the accumulation term in the gas phase is kept to derive the reduced model using the Liapunov–Schmidt technique.

A pseudo-homogenous model can be used for the solid phases (cases when $i = 2$ and 3). Since the interphase heat transport time is several orders of magnitude smaller than the typical residence time because of the very small pore size in the deposit layer, the gas and solid temperatures can be assumed to be equal. With the above assumptions, the energy equation in the deposit layer is given as:

$$[(1-\varepsilon_p)(\rho C_p)_p + \varepsilon_p(\rho C_p)_g]\ \frac{\partial T_2}{\partial t} + \varepsilon_p(\rho C_p)_g\ v_2 \frac{\partial T_2}{\partial x} = k_{ep}\left(\frac{\partial^2 T_2}{\partial z^2} + \frac{\partial^2 T_2}{\partial x^2}\right) + H'_{reaction}(y, T_2) \quad \text{(A2)}$$

and in the substrate wall:

$$[(1-\varepsilon_w)(\rho C_p)_w + \varepsilon_w(\rho C_p)_g]\ \frac{\partial T_3}{\partial t} + \varepsilon_w(\rho C_p)_g\ v_3 \frac{\partial T_3}{\partial x} = k_{ew}\left(\frac{\partial^2 T_3}{\partial z^2} + \frac{\partial^2 T_3}{\partial x^2}\right) \quad \text{(A3)}$$

Here, ε_p is the void fraction of the deposit layer, ε_w is the void fraction of the substrate wall, ρ represents density, C_p heat capacity, k_{ep} and k_{ew} are the effective thermal conductivities of the deposit layer and wall, and $H'_{reaction}$ $(y,T) = (-\Delta H)\ r_{reaction}\ (y,T)$ is the energy release per unit time per unit volume.

Equations A1–A3 can be combined into a general form

$$\alpha \frac{\partial^2 T}{\partial x^2} = \frac{\partial T}{\partial t} + u\frac{\partial T}{\partial z} - \alpha \frac{\partial^2 T}{\partial z^2} + \gamma\ v \frac{\partial T}{\partial x} + H' \quad \text{(A4)}$$

where, α is a vector of thermal diffusivities, given by

$$\alpha = \begin{cases} \dfrac{k_g}{(\rho C_p)_g}, & i = 1,4 \\ \dfrac{k_{ep}/(\rho C_p)_g}{(1-\varepsilon_p)\Gamma_p + \varepsilon_p}, & i = 2 \\ \dfrac{k_{ew}/(\rho C_p)_g}{(1-\varepsilon_w)\Gamma_w + \varepsilon_w}, & i = 3 \end{cases},$$

where $\Gamma_p = (\rho C_p)_p/(\rho C_p)_g$ is the thermal capacitance ratio of the particulate matter to the gas and $\Gamma_w = (\rho C_p)_w/(\rho C_p)_g$ is the thermal capacitance ratio of the substrate wall to the gas. In Eq. A4, γ is the heat capacity ratio of the different phases to the gas heat capacitance $(\rho C_p)_g$, and is given by

$$\gamma = \begin{cases} 1, & i = 1,4 \\ \dfrac{\varepsilon_p}{(1-\varepsilon_p)\Gamma_p + \varepsilon_p}, & i = 2 \\ \dfrac{\varepsilon_w}{(1-\varepsilon_w)\Gamma_w + \varepsilon_w}, & i = 3 \end{cases}$$

Furthermore, the source term H' is given by

$$H' = \begin{cases} -\dfrac{H'_{reaction}}{(1-\varepsilon_p)(\rho C_p)_p + \varepsilon_p(\rho C_p)_g}, & \text{otherwise } i = 2 \\ 0, \end{cases}$$

Finally, it is noted that $u_2 = u_3 = 0$.

The boundary conditions are:

$$\frac{\partial T_1}{\partial x} = 0 \quad \text{at } x = 0,$$
$$\frac{\partial T_4}{\partial x} = 0 \quad \text{at } x = 2h + w_b + w_s,$$
$$\frac{\partial T_2}{\partial z} = 0 \quad \text{at } z = 0 \text{ and } z = L,$$
$$\frac{\partial T_3}{\partial z} = 0 \quad \text{at } z = 0 \text{ and } z = L,$$
$$u_1 = 0 \quad \text{at } x = h,$$
$$u_4 = 0 \quad \text{at } x = h + w_b + w_s,$$
$$u_1 = 0 \quad \text{at } z = L,$$
$$u_4 = 0 \quad \text{at } z = 0,$$
$$v_1 = 0, \quad \text{at } x = 0,$$
$$v_4 = 0, \quad \text{at } x = 2h + w_b + w_s,$$
$$T_1 = T_{inlet}, \qquad u_1 = u_{inlet} \quad \text{at } z = 0$$

The initial conditions are $T_i = T_b$ when $t = 0$ for all z and x. Furthermore, there are the usual momentum, temperature, and heat flux continuity conditions at the interfaces. These equations are rendered dimensionless according to the procedure illustrated in the mathematical model section of the main text to give Eq. 1.

Manuscript received Nov. 1, 2006, and revision received Feb. 20, 2007.